ON THE BENEFITS OF ECO-FRIENDLY CHITOSAN/ZnO COMPOSITE

Marinescu Maria-Roxana [1], Buiu Octavian[1], Pachiu Cristina[1], Brîncoveanu Oana[1], Romanițan Cosmin[1], Suchea Mirela[1,2], Mărculescu Ovidiu[3]

[1] National Institute for Research and Development in Microtechnologies IMT-Bucharest, Erou Iancu Nicolae Str., 126A, 077190, Romania; roxana.marinescu@imt.ro; octavian.buiu@imt.ro; cristina.pachiu@imt.ro; oana.brincoveanu@imt.ro; cosmin.romanitan@imt.ro; mira.suchea@imt.ro;
[2] Center of Materials Technology and Photonics, School of Engineering, Hellenic Mediterranean University, 71410 Heraklion, Crete, Greece; mirasuchea@hmu.gr
[3] National Research and Development Institute for Food Bioresources – IBA Bucharest, 5th Ancuta Baneasa Str., 2nd District, Bucharest, 020323, Romania; ovidiu.marculescu@bioresurse.ro

ABSTRACT: Chitosan (CS) is one of the most abundant bio-polymers that can be found on the planet. It is a natural biopolymer obtained from crustaceans' shells. Because it has great advantages like the fact that it is bio-compatible, degradable, non-toxic, and has antimicrobial activity, it has been widely used in different applications: wound dressing, drug delivery, food packaging, water treatment etc. Adding zinc oxide (ZnO) nanoparticles to chitosan improves its antibacterial activity. Preliminary results of a study of the effect of ZnO addition (various concentrations) in chitosan-based composites are presented in this work. The exploration of chitosan/ZnO nanocomposites as sustainable materials is the subject of this paper.
KEYWORDS: Chitosan, ZnO, eco-friendly, bio materials

1. INTRODUCTION

Natural polymers have attracted special attention worldwide due to the extraordinary properties they possess. One of the most important properties of these polymers is biodegradability.

Natural polymers are abundantly found in bacteria, fungi, animals and plants [1]. These polymers include cellulose, chitin, collagen, silk, rubber, wool, amber, keratin, etc.

Chitin is a natural polymer that ranks second in distribution after cellulose. Chitin is very common in invertebrates or making up the exoskeleton of crustaceans, insects, and other arthropods. At the same time, it is a structural component of the cell wall of bacteria and fungi. It is insoluble in water and resistant to acids, bases, or most organic solvents. In crustaceans (ex. crab) it is impregnated with calcium carbonate for even greater hardness.

Due to the insolubility of chitin, it is not widely applicable so a deacetylation process in a strongly alkaline environment is done. This way is obtained the chitosan from chitin [2]. The properties of the chitosan, such as solubility, viscosity and biological activity are determined by the deacetylation degree (DD).

Chitosan is a biopolymer with antifungal, mucoadhesive, antibacterial and gelling properties [3], that has indeed been widely used across various fields due to its biocompatibility, biodegradability, and non-toxicity. Briefly, an overview of its applications is as following: medical and pharmaceutical applications (wound healing, drug delivery, tissue engineering); agriculture (plant growth, seed coating); food industry (preservation, edible film coatings); water treatment; cosmetics (skin care products, hair care).

Chitosan's versatility continues to drive research into new and innovative applications, with ongoing studies aiming to enhance its functionality and broaden its usage in different sectors. Some valuable studies of using chitosan are presented below, with given examples:

- **Food and Agriculture**

The main cause of food waste is the excessive purchase of products, fact that leads to the expiration of the validity period before being consumed. The use of chitosan in the food industry, such as a protective layer for vegetables or fruits, not only extends their shelf life but also helps reduce food waste. The global climate change is thought to be accelerated by the carbon dioxide produced by the wasted food. So, if the excess of food waste is reduced, it also brings benefits to global warming.

- Chitosan has been widely used to make edible films and coatings. These are thin, edible layers that serve as food coatings or protective barriers against the environment. For example, Khodaman E. et.al used in [4] chia mucilage-gelatine incorporated with chitosan nanoparticles to make such coatings for

food. Subramani G. and Manian R. combined chitosan with kaolin clay (KC) and bio-vanillin (BV) in order to create a novel antifungal and biodegradable food packaging film [5].
Some researchers studied the effects of chitosan for a certain fruit or aliment, like Dulta K. et al., which studied the impact of sodium alginate (SA), chitosan (CH) and nano zinc oxide (ZnO) layering on oranges [6]. Joshy K.S. et. al. made a novel zinc oxide reinforced xanthan gum hybrid system for edible coatings, that was tested on apples and tomatoes [7].

- **Medical field**

Skin is the largest organ of the body which, in optimal health conditions, regenerates itself every 27 days [8]. Any damage to the skin results in wounds. Wounds can be with or without tissue loss and acute or chronic, with the acute ones healing relatively faster [9].

Uncontrollable massive bleeding, haemorrhage, is often difficult to manage and becames a life threatening that can end up with the death of the patient.

Chitosan is effectively utilized in the wound healing process. It facilitates rapid haemostasis through electrostatic interactions between the amine groups in its molecular chain and the anions on the surfaces of red blood cell membranes and platelets [1].

To accelerate this process of healing, scientists used chitosan in different combinations.

Bakil S. et.al. used in [10] sodium alginate (SA) based ZnO nanoparticles as antibacterial film for wound healing applications.

Wang S. et.al. made a composite film consisting of eggshell membrane hydrolysate (ESMH), graphene oxide (GO) and chitosan (CS) to use for wounds [11].

In [12] the authors presented the chitosan (CS)/polyvinylpyrrolidone (PVP) sponges containing platelet-rich fibrin that they fabricated using the freeze drying method.

- **Environment**

All around the world, a large volume of wastewater is generated because of industrial development and urbanization. Obtaining new water treatment agents from pollutants such as dyes, heavy metals or drugs has become one of the most discussed topics of study among researchers.

Discovering the effects of chitosan, it is often used as a water treatment agent by different methods: by electrochemical method, separation with polymer membranes and by adsorption. For example, Dewsnelli D. et.al. used in [13] chitosan-ZnO composite to remove methylene blue when using the photodegradation method with the help of a UV lamp. Other researchers made membranes of chitosan and ZnO [14].

In [15] Meng Z. et.al. presented a chitosan-naphthylamide fluorescent probe for specific recognition and efficient adsorption of Hg^{2+}, a virulent heavy metal ion that leads to a serious threat to ecosystem and human health.

Chitosan has been used in several materials such as electrospun fibres, aerogels, hydrogels, microcapsules, and nanoparticles [3].
Chitosan in combination with ZnO, must bring a plus benefit regarding the antibacterial activity. Because of its unique thermal and mechanical qualities, zinc oxide has been studied for its potential use in wastewater treatment, antibacterial activity, gas sensing, catalysis, and magnetism [16].
This work regards a study of the effect of ZnO addition (in various concentrations) in chitosan-based composites.

2. METHODS AND MATERIALS

2.1 Materials

Chitosan for alimentary use was purchased from the local market without clear specification. Poly (acrylic acid) and Zinc oxide (ZnO) were both purchased from Sigma-Aldrich. The fibre glass tissue used in this research study was acquired from Jino company - https://www.jino.cz/ and carefully cleaned to remove any additives before use.

2.2 Methods

First, five probes were prepared using an exact quantity of materials. A fix amount of 50 mg of poly (acrylic acid) (PAA) was weighted and poured in 50 deionized water. Next, 0.5 g of chitosan were added and the solution was vigorously stirred for two hours using a magnetic stirrer. Next, different quantities of zinc oxide were added to the solutions: 0; 50; 150; 300 and 500 mg ZnO, solutions that were named P0; P1; P2; P3 and P4.

The final solutions were mixed by ultrasonication for one hour in a large „Elmasonic X-tra basic" ultrasonic bath in order to ensure the proper ZnO dispersion in the PAA – chitosan solution and prevent agglomerations [17].

The preparation steps are presented in Figure 1.

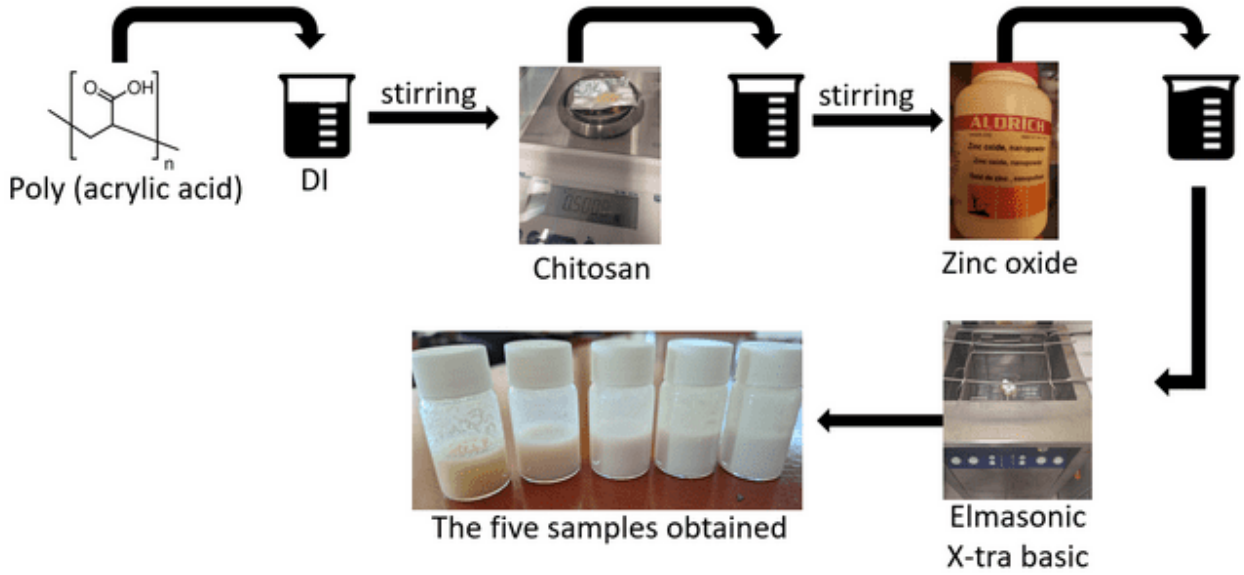

Figure 1. Preparation of Chitosan-ZnO composite

After obtaining the homogenous suspensions, three types of substrates were used for depositions: fabric, paper, and glass. Glass fibers are used as a stable substrate for composite material deposition. Glass fibres are often utilized in composite materials due to their advantageous properties, such as: mechanical strength, thermal stability, chemical resistance and lightweight. In a composite structure, glass fibres serve as a reinforcing phase, while the matrix material (often a polymer, resin, or metal) binds the fibres and transfers loads. The stability of glass fibres as a substrate ensures effective bonding with the matrix, promoting uniform stress distribution and enhanced mechanical performance in the final composite material. In this paper are presented the results obtained for the depositions on fiberglass First, a layer of each solution was brushed on the fiberglass fabric and the results can be seen in Table 2.

The concentrations of probes are presented in table 1:

Table 1. The concentration of probes

No	Deionized water (DI)	Poly (acrylic acid) (PAA)	Chitosan (CS)	Zinc oxide (ZnO)
P0	5 g	0.05 g	0.5 g	0 g
P1	5 g	0.05 g	0.5 g	0.05 g
P2	5 g	0.05 g	0.5 g	0.15 g
P3	5 g	0.05 g	0.5 g	0.30 g
P4	5 g	0.05 g	0.5 g	0.50 g

Table 2. Photos of the samples

	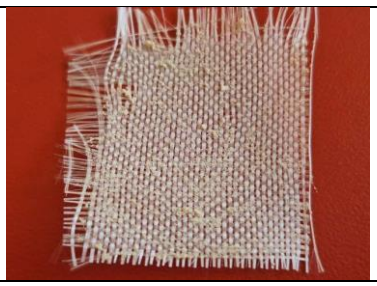	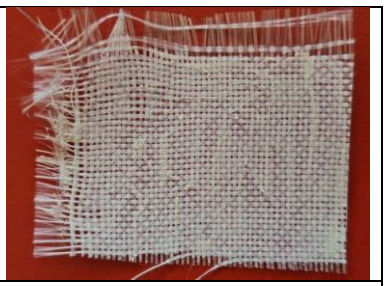
Fiberglass	Sample P0	Sample P1
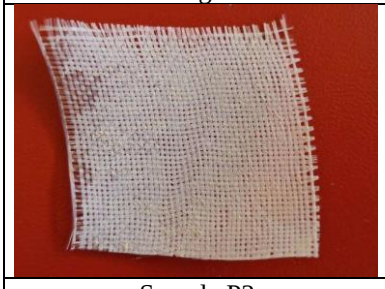	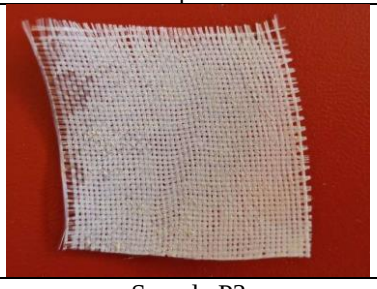	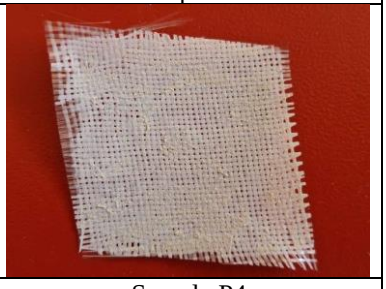
Sample P2	Sample P3	Sample P4

Fiberglass combined with chitosan deposition is an interesting topic that merges two complementary materials - fiberglass tissues for their strength and structural properties, and chitosan for its bioactive and functional qualities. Furthermore, a composite made of **fiberglass tissue, chitosan** and **zinc oxide (ZnO)** combines the best of each material-strength from fiberglass, antibacterial and biocompatible properties from chitosan, and antimicrobial and UV protection from ZnO. This combination has a high potential in applications such as biomedical devices, water treatment, and antibacterial surfaces.

3. RESULTS

3.1 Morphological analysis by Scanning Electron Microscopy (SEM)

The Field Emission Scanning Electron Microscope (FE-SEM) Nova NanoSEM 630 (FEI Company, USA), equipped with EDX detector (EDAX TEAM™, USA) from IMT Bucharest was used to analyze the structural properties of the composition deposited on the fiberglass fabric.

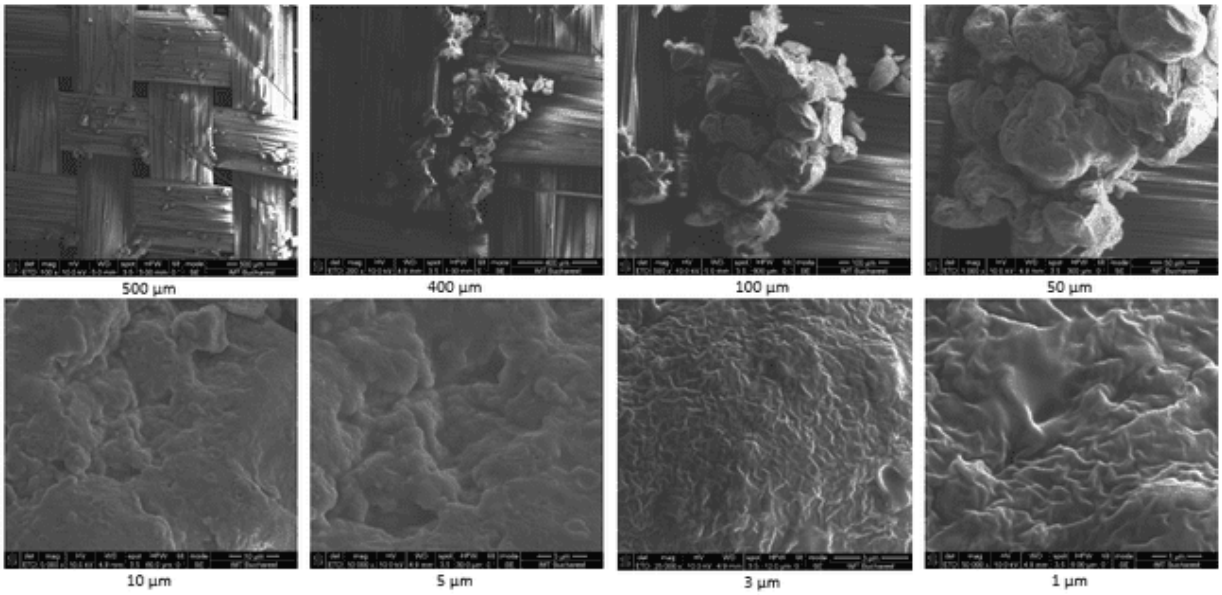

Figure 2. SEM images obtained at 500, 400, 100, 50, 10, 5, 3 and 1 µm reference size for probe P0

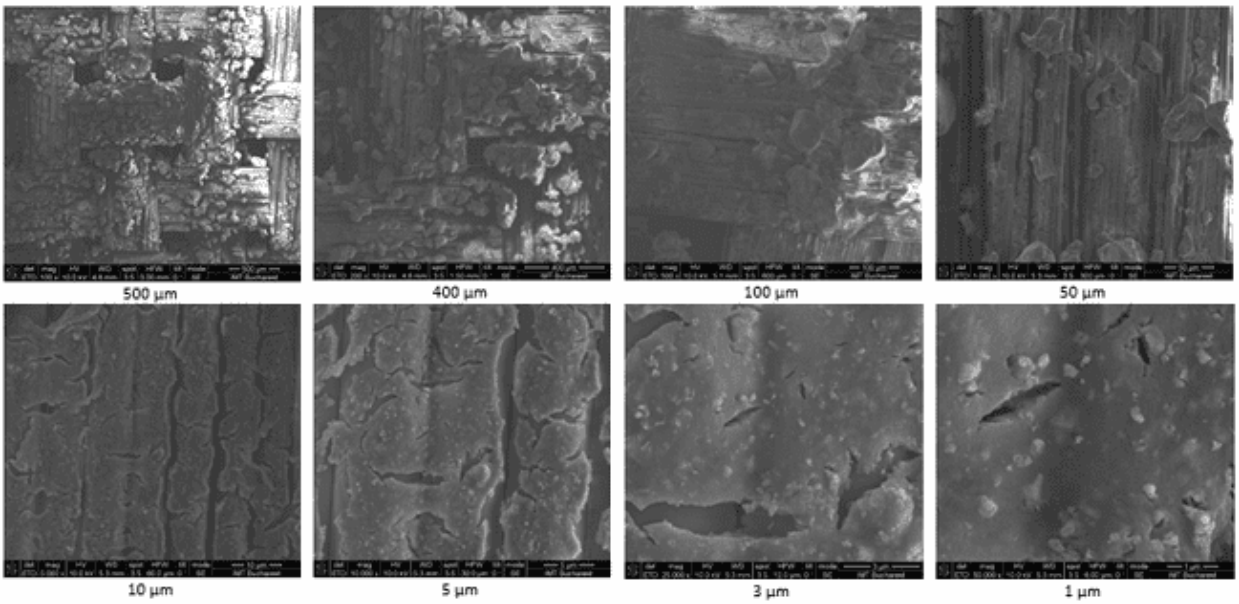

Figure 3. SEM images obtained at 500, 400, 100, 50, 10, 5, 3 and 1 µm reference size for probe P1

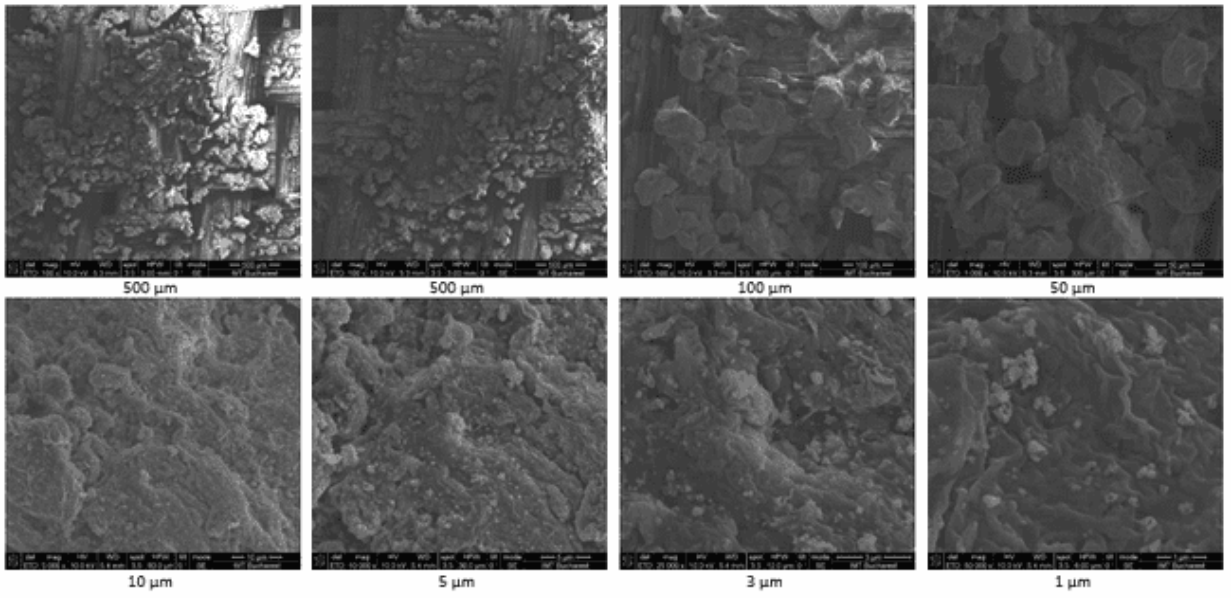

Figure 4. SEM images obtained at 500, 400, 100, 50, 10, 5, 3 and 1 µm reference size for probe P2

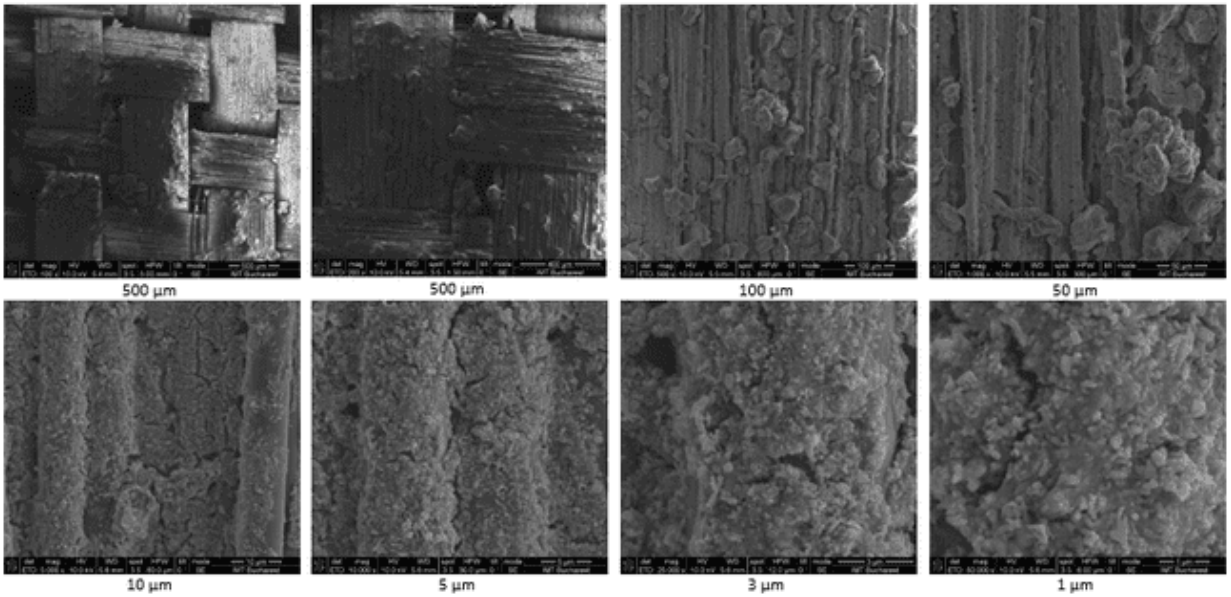

Figure 5. SEM images obtained at 500, 400, 100, 50, 10, 5, 3 and 1 µm reference size for probe P3

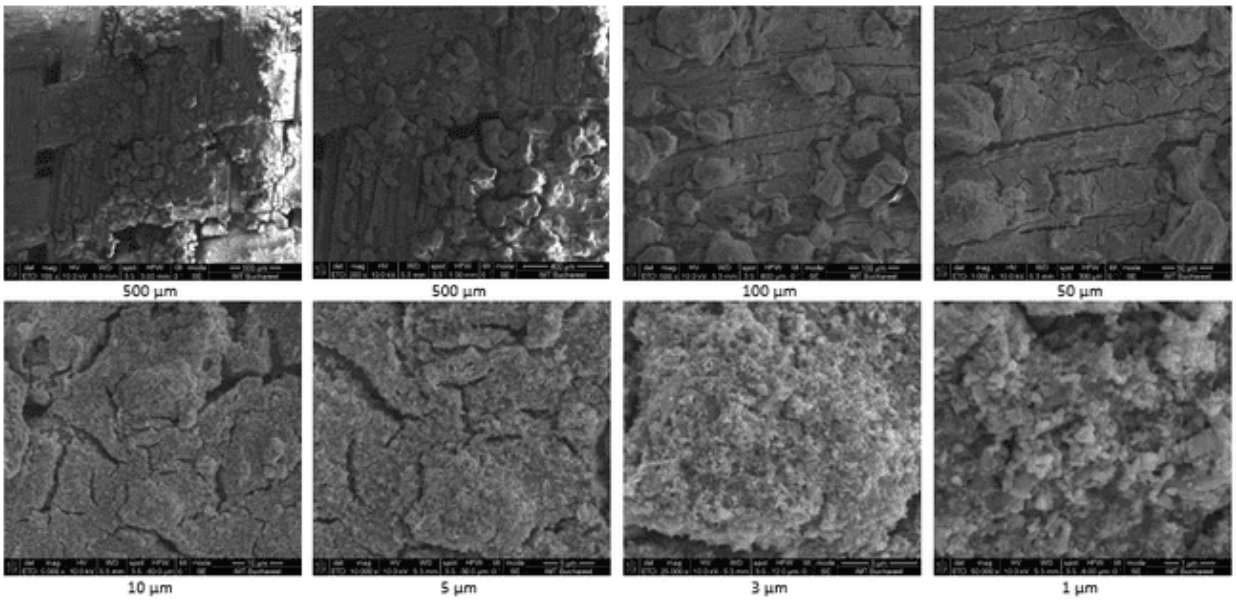

Figure 6. SEM images obtained at 500, 400, 100, 50, 10, 5, 3 and 1 µm reference size for probe P4

The SEM images contain detailed morphological data for the composite materials at various magnifications. A breakdown of the evaluation process based on the probes (P0–P4) follows:

General Morphology:

P0 (No ZnO): The surface of the chitosan-Poly(acrylic acid) (PAA) coating likely appears relatively smooth, with the texture primarily determined by the underlying fiberglass. Without ZnO, the coating may exhibit limited surface roughness, with few features for bacterial interaction. **P1 (Low ZnO)**: The addition of 0.05 g of ZnO likely introduces scattered small ZnO nanoparticles embedded within the chitosan matrix. These particles should be visible as minor surface irregularities, with increased surface roughness, providing initial contact points for potential bactericidal action. **P2 (Medium-Low ZnO)**: With 0.15 g of ZnO, particle aggregation likely starts to increase. The surface becomes rougher, with clusters of ZnO nanoparticles visible in the SEM images. These aggregates may enhance the bactericidal effect by increasing the surface area and creating more active sites for interactions with bacteria. **P3 (Medium ZnO)**: At 0.30 g of ZnO, the morphology shows even more pronounced aggregation. Larger clusters of ZnO nanoparticles would result in rougher surface textures, with a greater density of nanoparticles. This morphology could significantly improve bactericidal action, as more ZnO is exposed, promoting the generation of reactive oxygen species (ROS) that disrupt bacterial membranes. **P4 (High ZnO)**: With 0.50 g of ZnO, ZnO nanoparticles dominate the surface, possibly creating a highly uneven, coarse texture. At this concentration, ZnO likely covers much of the chitosan/PAA matrix, potentially leading to the highest bactericidal action in the series. However, excessive aggregation might reduce the overall surface area if clusters become too large, somewhat limiting ZnO exposure.

Effect of ZnO Concentration on Surface Morphology:

As ZnO concentration increases from P1 to P4, the surface morphology evolves from smooth to increasingly rough and textured, with larger and more frequent aggregates of ZnO nanoparticles. This roughness not only improves the physical interactions with bacterial cells but also enhances the release of Zn^{2+} ions and the production of ROS, both crucial for bactericidal activity.

Bactericidal Potential:

P0 (Control): Limited bactericidal activity, as there are no ZnO nanoparticles. The chitosan matrix may offer minimal antimicrobial properties, but not to the extent of ZnO.

P1 to P4: As ZnO concentration increases, the bactericidal effect should increase due to:

Direct contact:

Bacteria adhering to rougher surfaces face mechanical disruption.

ROS generation:

ZnO nanoparticles produce oxygen reactive species (ROS) upon exposure to light and moisture, damaging bacterial membranes.

Zn^{2+} ion release: These ions penetrate bacterial cell walls, disrupting their metabolic processes.

P3 and P4: These samples, with higher ZnO concentrations, are expected to exhibit the most potent bactericidal effects due to greater ZnO surface coverage and nanoparticle availability. However, over-aggregation in P4 might slightly reduce efficiency if nanoparticle clusters block ROS generation or ion release from certain areas.

This evaluation indicates that ZnO concentration has a strong influence on both the morphology and bactericidal action of the coatings, with a balance needed to prevent excessive aggregation from reducing surface effectiveness.

3.2 Raman analysis

Scanning Near-field Optical Microscope - Witec alpha 300S/Witec/2008 Witec Gmbh Germany was used for obtaining the Raman spectrums.

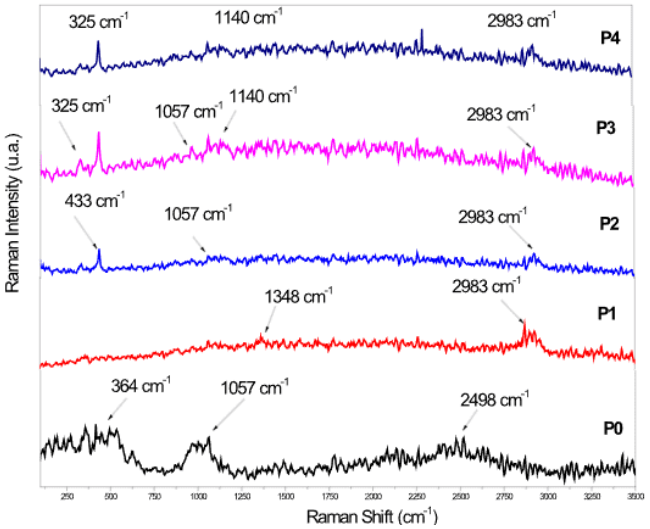

Figure 7. Raman images of the five samples

Peak Identification and Assignment: The Raman spectrum of each sample (P0 to P4) as it can be seen in figure 7 shows peaks corresponding to key components of the composite:

Chitosan:

Typical Raman peaks for chitosan can be found in the regions of 1000–1500 cm^{-1}, primarily due to C–C, C–O, and C–N stretching vibrations. You should

observe peaks around 1340 cm^{-1} (C–N stretching) and 1070 cm^{-1} (C–O stretching).

Poly (acrylic acid) (PAA):

Peaks around 1420–1450 cm^{-1} can be assigned to the carboxylate groups (COO^-) symmetric stretching of PAA, and around 1720 cm^{-1} for C=O stretching of the acid groups.

ZnO:

The presence of ZnO is indicated by the **E_2 (high)** mode typically seen around **437 cm^{-1}**, which corresponds to the wurtzite structure of ZnO. Additional modes like **A_1(TO)** and **E_1(LO)**, which appear around **330–380 cm^{-1}**, are also characteristic of ZnO nanoparticles. These peaks intensify as the concentration of ZnO increases.

Spectral Evolution with ZnO Concentration:

P0 (No ZnO): In the absence of ZnO, the Raman spectrum should only show the characteristic peaks of chitosan and PAA. There is no evidence of ZnO-related modes, and the spectrum is dominated by the organic matrix signals. **P1 (Low ZnO)**: As ZnO nanoparticles are introduced, you should begin to see weak intensity peaks related to the ZnO crystal structure, especially the **E_2 (high)** mode at 437 cm^{-1}. The organic peaks (chitosan and PAA) may still dominate, but ZnO peaks start to emerge. **P2 (Medium-Low ZnO)**: With more ZnO nanoparticles, the intensity of the ZnO-related peaks increases. The **E_2 (high)** mode becomes clearer, and you might also observe stronger peaks around 330–380 cm^{-1} (A_1(TO) or E_1(LO) modes). The presence of these peaks confirms the incorporation of ZnO within the composite and suggests better ZnO dispersion or exposure on the surface. **P3 (Medium ZnO)**: At 0.30 g of ZnO, the ZnO peaks should be even more prominent. The organic matrix peaks may still be present but could be partially overshadowed by ZnO signals. The intensity increase indicates greater ZnO coverage, correlating with SEM findings that show significant ZnO aggregation and surface roughness. **P4 (High ZnO)**: With the highest ZnO concentration, the Raman spectrum is expected to show dominant ZnO peaks, especially the **E_2 (high)** mode at 437 cm^{-1}. The organic peaks may become less prominent as ZnO takes over the surface. SEM images likely confirm this with high particle aggregation.

Correlation with SEM Observations:

P0 (No ZnO): SEM images show a smooth surface corresponding to the organic matrix. The Raman spectrum reflects this by showing no ZnO peaks and clear signals of chitosan and PAA. **P1 (Low ZnO)**: SEM shows small ZnO nanoparticles dispersed within the organic matrix. The Raman spectrum aligns with this, as ZnO peaks appear, but they are weak due to the low concentration and possible nanoparticle embedding in the matrix. **P2 (Medium-Low ZnO)**: As SEM images show more ZnO clusters, the Raman spectrum corroborates this by increasing ZnO peak intensity. The rougher surface seen in SEM likely exposes more ZnO to the surface, enhancing the Raman signal. **P3 (Medium ZnO)**: SEM shows larger ZnO aggregates, and the Raman spectrum intensifies correspondingly. The strong ZnO signals indicate that nanoparticles dominate the surface morphology, matching the SEM's depiction of rough, aggregated ZnO structures. **P4 (High ZnO)**: SEM reveals extensive ZnO aggregation, which is reflected in the Raman spectrum by dominant ZnO peaks. The organic matrix peaks fade as ZnO takes over, in line with the SEM's visual depiction of a highly textured surface.

Potential Bactericidal Action:

The evolution of ZnO-related Raman peaks and SEM-confirmed surface roughness strongly suggest that the bactericidal action increases with ZnO concentration. ZnO's ROS generation capacity is closely related to its exposure on the surface, which is well reflected in both SEM and Raman findings. P3 and P4, which show the most significant ZnO exposure and surface roughness, are likely to exhibit the highest bactericidal activity.

3.3 XRD analysis

SmartLab High Resolution Diffraction System/Rigaku Corporation, Japan, 2008 was used for the XRD analysis. The XRD was done only for the samples that have ZnO in their composition: P1, P2, P3 and P4 as presented in Figure 8.

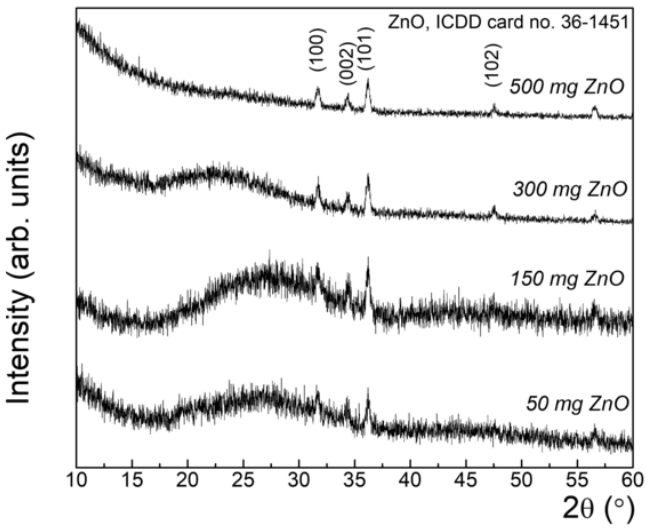

Figure 8. XRD graphic of the samples that contain ZnO

The XRD analysis shows diffraction peaks corresponding to both the organic chitosan matrix and the ZnO nanoparticles.

Chitosan:

A broad diffraction feature around **2θ = ~20°** is characteristic of amorphous chitosan. This peak corresponds to the disordered structure of the polysaccharide backbone, which lacks significant crystallinity. **ZnO**: The key peaks for ZnO in a wurtzite structure are observed at:

2θ = 32.1°: Assigned to the (100) reflection.

2θ = 34.6°: Assigned to the (002) reflection.

2θ = 36.2°: Assigned to the (101) reflection.

2θ = 47.2°: Assigned to the (102) reflection. These peaks correspond to the wurtzite ZnO crystal structure (ICDD card no. 36-1451), confirming the formation of ZnO nanoparticles in the composite.

Effect of ZnO Concentration on XRD Spectra:

P1 (Low ZnO): The ZnO peaks in P1 are relatively broad, indicating small crystallite sizes or less crystallinity of the ZnO nanoparticles. The broad nature of the peaks can also be attributed to the low ZnO concentration and potential interaction with the organic matrix (chitosan/PAA), which might hinder crystal growth. **P2 (Medium-Low ZnO)**: With an increase in ZnO concentration, the diffraction peaks become sharper and more intense, reflecting an increase in ZnO crystallite size and improved crystalline order. The (002) and (101) reflections at 34.6° and 36.2°, respectively, become more defined, indicating more significant particle growth compared to P1. **P3 (Medium ZnO)**: The ZnO peaks continue to sharpen, indicating further growth of ZnO crystallites. The increased intensity suggests higher ZnO content and greater crystal domain size. This is in line with the SEM observations of more prominent ZnO nanoparticle clusters. **P4 (High ZnO)**: The sharpest and most intense ZnO peaks are observed in this sample, reflecting the highest degree of crystallinity and the largest ZnO crystallite sizes. This observation correlates with the SEM results showing substantial ZnO nanoparticle aggregation on the surface.

Correlation with SEM and Raman Observations:

P1 (Low ZnO): The broad XRD peaks suggest small ZnO crystallites, which is consistent with the SEM observations showing dispersed ZnO nanoparticles within the matrix. The Raman spectrum for P1 shows weak ZnO peaks, reinforcing the idea that ZnO is present but in low concentrations and with minimal crystallinity. **P2 (Medium-Low ZnO)**: The sharpening of the ZnO peaks in XRD is consistent with both the SEM images (which show larger and more aggregated ZnO nanoparticles) and the Raman spectrum (where ZnO peaks become more intense). This indicates improved ZnO crystallinity and greater exposure of ZnO on the surface, enhancing its potential bactericidal effect. **P3 (Medium ZnO)**: The XRD data shows further crystallite growth, aligning with the SEM observations of larger ZnO aggregates and rougher surface morphology. The Raman spectrum for P3 also shows significant ZnO peaks, indicating that ZnO nanoparticles dominate both the morphology and chemical composition of the surface. **P4 (High ZnO)**: The sharp XRD peaks, prominent SEM-detected ZnO aggregates, and the strong ZnO peaks in the Raman spectrum together point to a high degree of ZnO crystallinity and concentration. The surface is densely covered with ZnO, which enhances the overall bactericidal activity as a result of the extensive crystalline domains capable of generating reactive oxygen species (ROS).

Crystallite Size Evolution:

The sharpening of ZnO peaks in the XRD data indicates an increase in crystallite size with higher ZnO concentration. This suggests that ZnO nanoparticles grow larger and form more crystalline domains as more ZnO is added to the composite. This observation is key because larger, more crystalline ZnO particles often exhibit enhanced bactericidal effects due to increased surface area and more efficient ROS generation.

Potential Bactericidal Action:

The crystallite size, surface roughness, and nanoparticle aggregation, as exposed by the XRD, SEM, and Raman analyses, together suggest the following: **P1 (Low ZnO)** has limited bactericidal action due to low ZnO crystallinity and minimal surface exposure. **P2 (Medium-Low ZnO)** shows increased bactericidal potential as ZnO crystallinity and surface exposure improve. **P3 (Medium ZnO)** and **P4 (High ZnO)**, with their larger crystallite sizes and greater surface coverage, should exhibit the most potent bactericidal effects due to increased ROS generation and better interaction with bacterial cells.

Chitosan role

Chitosan plays a crucial role in the composite structure across all samples in several ways:

Matrix Formation:

Mechanical Support:

Chitosan serves as the primary matrix material, providing mechanical stability and a medium for dispersing the ZnO nanoparticles. It also contributes to the film formation on the fiberglass substrate.

Interaction with ZnO:

Chitosan's amino groups can form interactions with ZnO nanoparticles, stabilizing them in the composite and preventing excessive aggregation at lower concentrations. This stabilization effect is crucial in lower-ZnO samples (P1 and P2), where ZnO is more finely dispersed.

Surface Characteristics:

P0 (No ZnO): Without ZnO, chitosan defines the surface morphology, which is smooth and lacking significant roughness. In this case, chitosan may exhibit limited antimicrobial properties due to its inherent bioactive nature but would be inferior compared to ZnO-enhanced samples. **P1 to P4 (ZnO-containing samples)**: As ZnO concentration increases, chitosan continues to act as the matrix, but the surface morphology is increasingly dominated by ZnO. However, chitosan remains crucial in providing the binding and structural support to hold the ZnO nanoparticles in place.

Antimicrobial Properties:

Chitosan itself possesses some antimicrobial properties, attributed to its ability to disrupt bacterial cell membranes and chelate metal ions, thereby hindering microbial growth. This property complements the bactericidal effects of ZnO. In samples with low ZnO concentration (P1 and P2), chitosan's bioactivity plays a more prominent role. However, in P3 and P4, ZnO's antimicrobial action becomes the dominant effect, although chitosan still enhances the overall efficacy through its synergistic interaction with ZnO.

XRD and Raman Observations:

XRD: The broad diffraction peak at 20° corresponding to chitosan is present in all samples, although it becomes less prominent as ZnO concentration increases and ZnO diffraction peaks dominate. This shows that chitosan is still a significant component of the composite but is increasingly overshadowed by ZnO in P3 and P4.

Raman: In the Raman spectra, the chitosan-related peaks around 1000–1500 cm^{-1} are present across all samples, with their intensity decreasing as ZnO content rises. This indicates that chitosan remains in the composite but has less of an influence on the surface chemistry as ZnO takes over.

Summary

P0 (No ZnO): Chitosan is the dominant component, contributing to the overall structure and offering limited bioactivity. **P1 and P2 (Low ZnO)**: Chitosan plays a dual role as a structural matrix and a bioactive agent, complementing the initial bactericidal effects of ZnO. **P3 and P4 (Higher ZnO)**: Chitosan's role is primarily as a stabilizing and binding matrix, while ZnO dominates both the surface morphology and the bactericidal action.

The fiberglass substrate acts as the **foundation** that provides mechanical support, enhances coating adhesion, and contributes to the overall structural integrity of the ZnO-chitosan composite. It plays an **indirect role** in the functional properties of the material (such as bactericidal action) by ensuring that the active ZnO and chitosan layers remain securely adhered to the surface and retain their morphology and effectiveness. Its high durability, chemical stability, and ability to support complex coatings make it a critical component of the composite system.

4. CONCLUSIONS

The combination of XRD, SEM, and Raman data provides a comprehensive view of the evolution of ZnO's structural, morphological, and chemical characteristics in the composites. As the ZnO concentration increases, there is a clear trend of enhanced crystallinity, larger particle size, and greater surface roughness, all of which contribute to stronger bactericidal activity. The analysis reveals that P3 and P4 is likely to be the most effective samples due to their larger ZnO crystallites and more exposed nanoparticle surfaces. In conclusion, chitosan acts as a scaffold that facilitates Zno nanoparticle distribution, contributes some intrinsic antimicrobial properties, and ensures the mechanical stability of the composite. However, as zno concentration increases, ZnO's impact on the composite properties, especially antimicrobial activity, becomes the dominant factor, with chitosan providing structural support in the background.

While the current materials show promise, further optimization can help maximize their performance for specific applications. Below are the steps to optimize the materials based on the desired outcomes: **Optimization for Antimicrobial Action**: Based on the analysis of SEM, Raman, and XRD, a balance must be struck between ZnO concentration and particle aggregation. High concentrations of ZnO (as in P4) lead to significant aggregation, which could reduce the surface area available for microbial interactions. Further experiments could optimize ZnO concentrations to maintain high antimicrobial activity while minimizing excessive aggregation. One next step would be to investigate ZnO concentrations between P2 and P3 to find the ideal balance between surface coverage and particle size for bactericidal efficacy. **ZnO Particle Size Control**: Smaller ZnO nanoparticles provide a higher surface area and more effective bactericidal action. Tailoring the synthesis method of ZnO could help reduce particle size and improve uniformity. One next step would be to investigate synthesis conditions that yield smaller, more uniform ZnO nanoparticles, such as using surfactants and controlling the pH during synthesis. **Chitosan Cross-linking**: While chitosan provides valuable antimicrobial properties, its solubility in acidic conditions or exposure to water can limit its stability. Cross-linking chitosan with agents like glutaraldehyde or using chitosan derivatives (e.g., carboxymethyl chitosan) could enhance its chemical

stability without sacrificing bioactivity. **Surface Treatment of Fiberglass**: The interaction between fiberglass and the coating could be further improved through surface treatment of the fiberglass, such as **plasma treatment** or applying a coupling agent (e.g., silane). This would enhance coating adhesion and improve the overall mechanical strength of the composite. **Antimicrobial Testing**: To confirm the antibacterial efficacy, quantitative microbial testing (e.g., zone of inhibition tests or colony counting) should be conducted. Testing under different conditions (UV exposure, varying pH, temperature) will give insights into the stability and performance of the composite. This ZnO-chitosan-fiberglass composite shows great promise, particularly in antibacterial applications, environmental remediation, and as protective coatings. By fine-tuning ZnO concentrations, improving surface adhesion, modifying chitosan, and optimizing the fiberglass substrate, the material can be further enhanced for a wide range of practical applications. Proper testing and validation will also help in realizing its full potential in targeted applications.

5. ACKNOWLEDGEMENTS

This work was supported partially by Romanian Ministry of Research, Innovation and Digitalization under the Romanian National Nucleu Programme – μNanoEl, project code PN 2307, contract no. 8N/03.01.2023 and by PNRR/2022/C9/MCID/I8 CF23/14 11 2022 contract 760101/23.05.2023 financed by the Ministry of Research, Innovation and Digitalization in "Development of a program to attract highly specialized human resources from abroad in research, development, and innovation activities" within the – PNRR-IIIC9-2022 – 18 PNRR/2022/Component 9/investment8.

6. REFERENCES

1. Xiaowei H., Yankun Z., Jinfa M., Xin N., Shumeng B., Natural polymer-based bioadhesives as hemostatic platforms for wound healing, *International Journal of Biological Macromolecules,* 256(1), pp. 128275, (2024).
2. Shadpour M., Fariba S., Chaudhery M. H., A journey to the world of fascinating ZnO nanocomposites made of chitosan, starch, cellulose, and other biopolymers: Progress in recent achievements in eco-friendly food packaging, biomedical, and water remediation technologies, *International Journal of Biological Macromolecules*, Vol. 170, pp. 701-716, (2021).
3. Sharkawy A., Barreiro M.F., Rodrigues A.E., Chitosan-based Pickering emulsions and their applications: A review, *Carbohydrate Polymers,* 250, pp. 116885 (2020).
4. Khodaman E., Barzegar H., Jokar A., Jooyandeh H., Production and evaluation of Physicochemical, Mechanical and Antimicrobial Properties of Chia (Salvia hispanica L.) mucilage-gelatin based Edible Films Incorporated with Chitosan Nanoparticles, *Journal of Food Measurement and Characterization*. 16, pp. 3547-3556, (2022).
5. Subramani G., Manian R., Bioactive chitosan films: Integrating antibacterial, antioxidant, and antifungal properties in food packaging, *International Journal of Biological Macromolecules,* 278(1), pp. 134596, (2024).
6. Dulta, K., Koşarsoy Ağçeli, G., Thakur, A. *et al.* Development of Alginate-Chitosan Based Coating Enriched with ZnO Nanoparticles for Increasing the Shelf Life of Orange Fruits (*Citrus sinensis* L.). *J Polym Environ* **30**, 3293–3306 (2022).
7. Joshy K.S., Jiya Jose, Tianduo Li, Merlin Thomas, Aruna M. Shankregowda, Sreejith Sreekumaran, Nandakumar Kalarikkal, Sabu Thomas, Application of novel zinc oxide reinforced xanthan gum hybrid system for edible coatings, *International Journal of Biological Macromolecules,* Vol. 151, pp. 806-813, (2020).
8. Yousef H, Alhajj M, Fakoya AO, et al. Anatomy, Skin (Integument), Epidermis. [Updated 2024 Jun 8]. In: StatPearls [Internet]. Treasure Island (FL): StatPearls Publishing; 2024 Jan-. Available from: https://www.ncbi.nlm.nih.gov/books/NBK470464/
9. Rezaie F, Momeni-Moghaddam M, Naderi-Meshkin H. Regeneration and Repair of Skin Wounds: Various Strategies for Treatment. *The International Journal of Lower Extremity Wounds*.;18(3), pp. 247-261, (2019).
10. Wang S., Li X., Zhang Y., Abou-Elsoud M., Uk Ahn D., Shu D., Liu M., Huang X., Eggshell membrane hydrolysate incorporated GO/CS as an novel dressing for promoting wound healing in vivo, *Food Bioscience*, Vol. 61, pp. 104699, (2024).

    Bakil S. N. A., Kamal H., Abdullah H. Z., Idris M. I., Sodium Alginate-Zinc Oxide Nanocomposite Film for Antibacterial Wound Healing Applications, *Biointerface Research in Applied Chemistry,* 10(5), pp. 6245-6252, (2020).

11. Mohamadreza, T., Marjan, M., Sheyda, L., Jaleh, V., Somayeh, T., Franoosh, J., Saeedeh, S., Shaghayegh, A., Azadeh, S., Fabrication and evaluation of Cs/PVP sponge containing platelet-rich fibrin as a wound healing accelerator: An in vitro and in vivo study, *International Journal of Biological Macromolecules*, 204, pp. 245-257, (2022).
12. Desnelli, D., Yulinda, L., Fernando, D., Fatma, F., Mara, A., Said, M., Chitosan-ZnO composite for removal of methylene blue, Indonesian J. *Fundam. Appl.Chem.*, 8(3), pp. 133-138, (2023).
13. Spoială A., Ilie C-I., Dolete G., Trușcă R-D., Motelică L., Oprea O-C, Ficai D., Ficai A., Andronescu E., Dițu L-M., The development of antimicrobial chitosan/ZnO nanocomposite membranes for water purification, *Romanian Journal of Materials*, 52 (1), pp. 17- 25, (2022).
14. Meng Z., Li X., Liang Y., Gu Y., Xu X., Wang Z., Yang Y., Wang S., An efficient chitosan-naphthalimide fluorescent probe for simultaneous detection and adsorption of Hg2+ and its application in seafood, water and soil environments, *International Journal of Biological Macromolecules*, Vol. 247, pp. 125807, (2023).
15. Akhter S.M.H., Siddiqui V.U., Ahmad S., Husain D., Naeem S., Alam M.T., Sustainable synthesis of zinc oxide nanoparticles using Terminalia chebula extract: Effect of concentration and temperature on properties and antibacterial efficacy, *Nano-Structures & Nano-Objects*, 38, pp. 101158, (2024).
16. Abolfazl D., Javad K.-S., Mohammad A. Mo., Sonochemical synthesis of novel decorated graphene nanosheets with amine functional Cu-terephthalate MOF for hydrogen adsorption: Effect of ultrasound and graphene content, *International Journal of Hydrogen Energy*, 44 (48), pp. 26444-26458, (2019).